

SCATPI, A Subroutine for Calculating π N Cross Sections and Polarizations for Incident Pion Kinetic Energies Between 90 and 300 MeV

John B. Walter*
Glen A. Rebka, Jr.*

NOTICE
This report was prepared as an account of work
sponsored by the United States Government. Neither the
United States nor the United States Department of
Energy, nor any of their employees, nor any of their
contractors, subcontractors, or their employees, makes
any warranty, express or implied, or assumes any legal
liability or responsibility for the accuracy, completeness,
or usefulness of any information, apparatus, product, or
process disclosed, or represents that its use would not
infringe privately owned rights.

*Guest Scientists. Physics Department, University of Wyoming, Laramie, WY 82070.



SCATPI, A SUBROUTINE FOR CALCULATING π N CROSS SECTIONS AND
POLARIZATIONS FOR INCIDENT PION KINETIC ENERGIES BETWEEN 90 AND 300 MeV

by

John B. Walter and Glen A. Rebka, Jr.

ABSTRACT

A subroutine, SCATPI, has been written which calculates π^+p and π^-p elastic differential cross sections for incident pion kinetic energies between 90 and 310 MeV for π^+p and 88 and 290 MeV for π^-p . The calculation is based upon the phase shift analysis of Carter, Bugg, and Carter, and is reliable to about 2% for π^+p and 3% for π^-p differential cross sections. SCATPI also calculates other scattering parameters for the π^+p systems. The calculations are compared with the measurements used in the phase shift analysis, and with selected recent measurements. The use of SCATPI is described.

I. INTRODUCTION

An estimate of the pion-nucleon elastic scattering amplitude, cross sections, and other scattering parameters at a given energy and angle which has been derived from the best experimental measurements available can be useful for both theory and experiment. Such estimates are often used for input to theoretical calculations of the interaction of pions with complex nuclei or for normalizing experimental data from pion beams to the "measured" elastic cross section. We have constructed a subroutine, SCATPI, which calculates these quantities for $\pi^\pm p$ elastic scattering with kinetic energies between 90 and 300 MeV at any angle. The subroutine was derived from the phase shift analysis of Carter, Bugg, and Carter¹ which in turn had been based primarily on the differential cross sections for $\pi^\pm p$ elastic scattering measured by Bussey, Carter, Dance, Bugg, Carter, and Smith,² but also on total cross sections, integrated charge exchange cross sections and polarization measurements.^{3,4,5,6} Their analysis provided eleven sets of phase

shifts for the π^+p system between 95 and 310 MeV, and nine for the π^-p system between 89 and 292 MeV. These were fitted by least squares to plausible functions of momentum, which had as few free parameters as would permit a reasonable χ^2/ν . Thus the phase shifts interpolated with these functions should be physically reasonable.

As a minimum test of its accuracy, the predictions of SCATPI have been compared to the measurements from which it was derived and have typically differed by the following amounts:

	π^+p	π^-p
differential elastic cross section	2%	2½% below 260 MeV 4% above 260 MeV
total cross section	½%	1%
integrated charge exchange cross sections	---	1%

These differences are generally reasonable considering the uncertainties in the measurements, except for the π^-p elastic differential cross section at higher energies where the phase shift analysis seems in some difficulty. Predictions for the polarization parameter also agree reasonably with the measurements. Predictions of SCATPI have also been compared to measurements that have become available since the subroutine was completed, and have agreed generally. Of course, deviations do occur where the old and new measurements are not fully compatible. As the performance of SCATPI does vary from energy to energy and angle to angle, a potential user should compare the predictions of SCATPI with measurements in the particular region of interest to determine the uncertainty which might be anticipated. Both the subroutine SCATPI and the program CROSSEX which compares the calculated predictions to measurement are available from the authors in FORTRAN decks with listings. These have been used with CDC 6600's and 7600's at the Los Alamos Scientific Laboratory and with the Xerox Sigma 7 at the University of Wyoming, and should be adaptable for any FORTRAN compiler.

II. COMPUTATIONAL SCHEME

SCATPI is based upon a set of phase shifts that are interpolated from the analysis of Carter, Bugg and Carter,¹ and necessarily follows the same scheme employed by those authors in relating the phase shifts to the cross sections and other scattering parameters. This section explains this scheme and details the interpolation of the phase shifts.

The scattering of a spin 0 particle from a spin $\frac{1}{2}$ particle is treated in many texts. When angular momentum and parity are conserved, the most general scattering amplitude in the center of momentum is

$$F = f(\theta, k) + g(\theta, k) \hat{n} \cdot \vec{\sigma} . \quad (1)$$

Here $\vec{\sigma}$ are the usual Pauli matrices, θ is the angle between the initial and final wave vectors, \vec{k}_i and \vec{k}_f , respectively, $k = |\vec{k}_i|$ is the initial wave number, and \hat{n} is a unit vector orthogonal to both \vec{k}_i and \vec{k}_f , $\hat{n} = \vec{k}_f \times \vec{k}_i / |\vec{k}_f \times \vec{k}_i|$. The functions $f(\theta, k)$ and $g(\theta, k)$ are commonly called the spin-nonflip and spin-flip scattering amplitudes, respectively. If the spin of the final state is not observed, the differential cross section is

$$\frac{d\sigma}{d\Omega} = |f(\theta, k)|^2 + |g(\theta, k)|^2 + 2 \operatorname{Re} [f^*(\theta, k) g(\theta, k)] \hat{n} \cdot \vec{P}_i , \quad (2)$$

where \vec{P}_i is the polarization, expectation value of $\vec{\sigma}$, for the initial state. If $|\vec{P}_i| = 0$, the differential cross section is

$$\frac{d\sigma}{d\Omega} = |f(\theta, k)|^2 + |g(\theta, k)|^2 \quad (3)$$

and the polarization of the final state is

$$\vec{P}_f = P_n \hat{n} = \frac{2 \operatorname{Re} [f^*(\theta, k) g(\theta, k)]}{|f(\theta, k)|^2 + |g(\theta, k)|^2} \hat{n} . \quad (4)$$

Measuring the differential cross section and the final state polarization for an unpolarized initial state yields the same information as measuring the differential cross section for a polarized initial state, as an examination of Eq. (2,3, 4) reveals. Measurement of the final state polarization in the latter case provides no additional information.

Since the Coulomb interaction with its long range cannot be ignored when both the pion and nucleon are charged, many terms must be kept in a partial wave expansion to adequately represent the resulting scattering amplitude; however, only a few contain significant contribution from the strong interaction. This difficulty can be avoided by separating from each partial wave an amount equal

to the partial wave for pure Coulomb scattering and by summing these pieces to the pseudo closed form discussed below. The scattering amplitudes are then written as

$$f(\theta, k) = f_C(\theta, k) + f_N(\theta, k) \quad (5)$$

$$g(\theta, k) = g_C(\theta, k) + g_N(\theta, k) \quad ,$$

where f_C and g_C are the Coulomb amplitudes. f_N and g_N are the remainders of the scattering amplitudes, which are largely due to the strong interaction and should contain few partial waves.

The Coulomb amplitudes and phase shifts used in SCATPI are

$$\begin{aligned} f_C^\pm = & \mp (1-t)^{-4} \frac{\alpha}{1-\cos\theta} \left\{ \frac{1}{k\beta} \exp \left[\mp \frac{i\alpha}{\beta} \ln \frac{1-\cos\theta}{2} \right] \right. \\ & + \frac{1}{2(E_\pi + E_p)} \left[\frac{E_\pi + E_p - M}{E_p - M} + \frac{E_\pi + E_p + M}{E_p + M} \cos\theta - (\mu_p - 1) \frac{E_\pi}{M} (1-\cos\theta) \right. \\ & \left. \left. - (\mu_p - 1) \frac{E_p - M}{2M} \sin^2\theta \right] - \frac{1}{k\beta} \right\} \end{aligned} \quad (6a)$$

$$\begin{aligned} g_C^\pm = & \pm (1-t)^{-4} \frac{\alpha \sin\theta}{2(E_\pi + E_p)(1-\cos\theta)} \left[\frac{E_\pi + E_p + M}{E_p + M} + (\mu_p - 1) \frac{2E_\pi + E_p + M}{2M} \right. \\ & \left. + (\mu_p - 1) \frac{E_p - M}{2M} \cos\theta \right] \end{aligned} \quad (6b)$$

$$v_1^\pm = v_0^\pm \pm \frac{\alpha}{\beta} \frac{1}{3\kappa} \{1 - (1+\kappa)^{-3}\} \quad (7a)$$

$$v_2^\pm = v_0^\pm \pm \frac{3\alpha}{2\beta} \frac{1}{3\kappa^2} \{2\kappa - 1 + (1+\kappa)^{-2}\} \quad (7b)$$

$$v_3^\pm = v_1^\pm \pm \frac{5\alpha}{6\beta} \frac{1}{\kappa^3} \{4 - 3\kappa + 2\kappa^2 - (4+5\kappa)(1+\kappa)^{-2}\} \quad , \quad (7c)$$

where f_C^+ , g_C^+ , and v_ℓ^+ apply for like charges while f_C^- , g_C^- and v_ℓ^- apply for opposite charges. Equations (6) are constructed from the exact nonrelativistic

solution for point charges, an additive relativistic correction to first order in α ,⁷ the fine structure constant, and a multiplicative form factor $(1-t)^{-4}$, which describes the charge distributions.¹ Equations (7) are derived from Eq. (6) after deleting the magnetic moment terms and ignoring the spin-flip amplitude, both of which are good numerical approximations.¹ Here $t=-\frac{1}{2}\kappa(1-\cos\theta)$ is the square of the momentum transfer, and $\kappa=(2\chi_\rho k)^2$ with $\chi_\rho=0.2563$ fm the Compton wavelength of the ρ -meson. E_π and E_p are the total energies of the pion and proton, respectively, in the center of momentum systems, while M is the proton rest energy, all in units of $\hbar c$. In Eq. (6) μ_p is the proton magnetic moment in nuclear magnetons. β is the laboratory velocity of the incident pion over c .

The amplitudes f_N and g_N can be expanded in partial wave series as

$$f_N(\theta, k) = \sum_{\ell=0}^{\infty} \exp(i\epsilon v_\ell) [(\ell+1)A_{\ell+}(k) + \ell A_{\ell-}(k)] P_\ell^0(\cos\theta). \quad (8a)$$

$$g_N(\theta, k) = \sum_{\ell=1}^{\infty} \exp(i\epsilon v_\ell) [A_{\ell+}(k) - A_{\ell-}(k)] P_\ell^1(\cos\theta). \quad (8b)$$

Here $\epsilon=2$ for elastic scattering and $\epsilon=1$ for charge exchange scattering, $A_{\ell\pm}$ are the partial wave amplitudes for total angular momentum $j=\ell\pm\frac{1}{2}$, and P_ℓ^0, P_ℓ^1 are the associated Legendre functions. Only a few terms contribute to these sums due to the short range of the strong interaction. For energies below about 300 MeV, Carter, Bugg and Carter find that only terms with $\ell \leq 3$ are important. For charge exchange scattering, f_N and g_N are the complete scattering amplitudes since the Coulomb amplitudes vanish, and SCATPI calculates the differential cross section and recoil neutron polarization using f_N, g_N from Eq. (8) in Eq. (3,4). For $n^{\pm}p$ elastic scattering, SCATPI calculates the differential cross section and polarization without Coulomb scattering using Eq. (8) in Eq. (3,4), or includes Coulomb scattering by summing Eq. (6) and Eq. (8) for the complete scattering amplitudes and using these sums in Eq. (3,4). SCATPI also calculates the integrated cross section.

$$\sigma_I = 4\pi \sum_{\ell=0}^{\infty} \frac{1}{2\ell+1} [|(\ell+1) A_{\ell+} + \ell A_{\ell-}|^2 + \ell(\ell+1) |A_{\ell+} - A_{\ell-}|^2] \quad (9)$$

and, from the optical theorem, the total cross section

$$\sigma_T = \frac{4\pi}{k} \sum_{\ell=0}^{\infty} \text{Im} [(\ell+1)A_{\ell+} + \ell A_{\ell-}] , \quad (10)$$

which if necessary exclude Coulomb scattering since the Coulomb amplitudes are divergent at $\theta=0$.

The strong interaction between pions and nucleons, which have isospin 1 and $\frac{1}{2}$, respectively, is thought to depend only on the total isospin I and not on orientation in its space. If this were the only coupling operative, states of total isospin would be eigenstates and scattering amplitudes for the several pion-nucleon charge states would be linear combinations of those amplitudes for $I=\frac{3}{2}$ and $3/2$ times the appropriate products of Clebsch-Gordon coefficients. The electromagnetic interaction, however, conserves only I_3 , not I , and thus perturbs this simple description. Some of the better understood charge dependent effects are explicitly isolated when the partial wave scattering amplitudes are written in the following form, which was used by Carter, Bugg, and Carter.

$$A_{\ell\pm} (\pi^+ p \rightarrow \pi^+ p) = \frac{1}{2ik} \{ \exp[2i(\delta_{3\ell\pm} + C_{3\ell\pm})] - 1 \} \quad (11a)$$

$$A_{\ell\pm} (\pi^- p \rightarrow \pi^- p) = \frac{1}{2ik} \left\{ \frac{2}{3} \exp[2i(\delta_{1\ell\pm} - \frac{2}{3} C_{1\ell\pm})] \right. \\ \left. + \frac{1}{3} \exp[2i(\delta_{3\ell\pm} - \frac{1}{3} C_{3\ell\pm})] - 1 \right\} \quad (11b)$$

$$- \frac{4}{9k} C_{13\ell\pm} \exp[i(\delta_{1\ell\pm} + \delta_{3\ell\pm})]$$

$$A_{\ell\pm} (\pi^- p \rightarrow \pi^0 n) = \sqrt{\frac{k'}{k}} \left\{ \frac{\sqrt{2}}{3} \frac{1}{2ik} \{ -\exp[2i(\delta_{1\ell\pm} - \frac{2}{3} C_{1\ell\pm})] \right. \\ \left. + \exp[2i(\delta_{3\ell\pm} - \frac{1}{3} C_{3\ell\pm})] \right\} \quad (11c) \\ \left. - \frac{\sqrt{2}}{9k} C_{13\ell\pm} \exp[i(\delta_{1\ell\pm} + \delta_{3\ell\pm})] \right\}$$

Subscripts 1 and 3 refer to isospin $\frac{1}{2}$ and $\frac{3}{2}$ respectively. The factor $\frac{k'}{k}$ in Eq. (11c), in which k' is the wave number in the $\pi^0 n$ final state, describes the increase in phase space due to the change in rest masses. In a potential model, joint action of the Coulomb and strong interaction potentials creates charge dependent phase shifts given by $C_{1\ell\pm}$ and $C_{3\ell\pm}$.⁸ It also adds charge dependent terms scaled by $C_{13\ell\pm}$ to the scattering amplitudes with $I_3 = \pm \frac{1}{2}$, because total isospin is no longer conserved. The remainder of the phase shift δ is caused mostly by the strong interaction; however it may still depend on the charge states in several ways. The elasticity, $\exp(2 \text{Im}(\delta))$, reflects loss to other channels, which may well depend on the charge state. For the energies considered here, elasticities with $I=3/2$ differ for $\pi^+ p$ and $\pi^- p$ initial states because a γn final state is available for the $\pi^- p$ initial state. They may also depend on the final state as well. A term given by

$$\Delta\eta = \frac{4}{3} \frac{k'-k}{k} \sin^2(\text{Re}(\delta_{3,1+})) \quad (12)$$

must be added to the P_{33} elasticity when $\pi^- p$ goes to the $\pi^0 n$ final state which has a different total rest mass from the initial state. The $\text{Re}(\delta)$ may also depend on the charge state through electromagnetic effects which have not been explicitly isolated. Charge dependence in the location and width of resonances in the strong interaction would be an interesting example of such effects.

The phase shift δ used in SCATPI are interpolated from those found in the energy independent analysis of Carter, Bugg, and Carter, who use the formulation described above. Plausible functions of momentum that have been fitted to the eleven sets of phase shifts for $\pi^+ p$ and the nine sets for $\pi^- p$ generate estimates of the phase shifts for all energies between 100 and 300 MeV. Proper selection of functions which automatically fulfill known theoretical constraints and contain as few unknown parameters as possible is crucial for efficient use of the experimental information and for physically reliable interpolation. Nearly all contributions to δ are expected to have short range since the pure Coulomb scattering amplitude has been explicitly isolated and removed. To good approximation, therefore, δ will have the momentum dependence⁹

$$\tan \delta_\ell = k^{2\ell+1} V(k^2) \quad (13)$$

The interpolation functions must have this form. For the P_{33} phase shift, the function includes a polynomial term in addition to a modified Breit-Wigner resonance

$$\delta = k^3 \sum_{m=0}^N a_m k^{2m} + \arctan \frac{\Gamma_{el}(k)}{2(E_r - E) - i\Gamma_{in}(k)} . \quad (14)$$

Here E is the total center of momentum energy, E_r is the rest energy of the resonance, and Γ_{el} and Γ_{in} are the elastic and inelastic widths of the resonance. The elastic width has the form given by Jackson¹⁰

$$\Gamma_{el} = \Gamma_r \left(\frac{2E_r}{E_r + E} \right) \left(\frac{k}{k_r} \right)^3 \frac{1 + (R k_r)^2}{1 + (Rk)^2} \quad (15)$$

with k_r the wave number at resonance, and Γ_r and R are constants. The inelastic width is approximated as constant for $\pi^- p$ and zero for $\pi^+ p$. The a_m are also constants. For the P_{11} phase shifts, the function also has the form of Eq. (14) for we wished to model the P_{11} inelasticity as arising through the $N(1470)$ resonance although only the tail of this resonance is in the energy range of interest. The elastic width has the form of Eq. (15) but with $R=0$. Since the inelasticity is believed to be largely in the pion production channel, the inelastic width has the form

$$\begin{aligned} \Gamma_{in} &= 0, & E < E_t, \\ &= b (E - E_t)^2, & E \geq E_t, \end{aligned} \quad (16)$$

with E_t the threshold for pion production and b a constant. For the remaining phase shifts, the functions have the form

$$\delta_\ell = k^{2\ell+1} \sum_{m=0}^N a_m k^{2m}. \quad (17)$$

In Eq. (14,17) the constants a_m carry the same subscripts as δ , so that, for instance, $a_{m,3,1-}$ are associated with $\delta_{3,1-}$, the P_{31} phase shift. Each phase shift was fit to the appropriate form, Eq. (14) or Eq. (17), for several trial values of N . SCATPI interpolates δ_i , i indicating all of the subscripts, using the parameter values obtained with the smallest value of N_i for which a reasonable

χ^2/ν was achieved. Tables I-II list respectively the real and imaginary parts of the a_m , while the resonance parameters are listed in Table III. Following Carter, Bugg, and Carter, the imaginary parts of the phase shifts are zero for π^+p . Similarly, the real part of the P_{33} phase shift is also charge dependent. Since only the low energy tail of the $N(1470)$ resonance lies in the energy range of interest, the width and rest energy were taken from the "Review of Particle Properties"¹¹ and not treated as free parameters. E_t was assigned the value 6.157 fm^{-1} . The S_{11} phase shift at 310 MeV precluded a reasonable solution for the $a_{m,1,0+}$, and therefore was ignored.

The calculation of C_1 , C_3 and C_{13} involves five numerical integrations for each value of l^\pm . For convenience, they are interpolated from the values used by Carter, Bugg, and Carter. These quantities depend on the strong as well as

TABLE I
REAL PART OF POLYNOMIAL PARAMETERS FOR THE PHASE SHIFTS^a

<u>Initial State</u>	<u>Spectroscopic Notation</u>	<u>$2I, l^\pm$</u>	<u>$\text{Re}(a_0)$</u>	<u>$\text{Re}(a_1)$</u>	<u>$\text{Re}(a_2)$</u>
	S_{11}	1,0+	9.5464	-	-
	P_{11}	1,1-	-6.1009	2.5928	-
	P_{13}	1,1+	-2.0870	0.4606	-
	D_{13}	1,2-	0.4706	-	-
	D_{15}	1,2+	0.7268	-0.4659	0.0925
	F_{15}	1,3-	0.0704	-0.0181	-
	S_{31}	3,0+	-6.4878	-7.5756	1.9960
	P_{31}	3,1-	-4.6544	1.0636	-
π^+p	P_{33}	3,1+	1.3270	-	-
π^-p	P_{33}	3,1+	-0.2806	-	-
	D_{33}	3,2-	0.2270	-0.1247	0.0172
	D_{35}	3,2+	-0.5524	0.3484	-0.0701
	F_{37}	3,3+	0.1334	-0.0466	-

^aThe a_i are in units of degrees times fm to the appropriate power. $\delta_{1,3+}$ and $\delta_{3,3-}$, not listed, are zero.

TABLE II

IMAGINARY PART OF POLYNOMIAL PARAMETERS FOR THE PHASE SHIFTS^a

Initial State	Spectroscopic Notation	$2I, l\pm$	$\text{Im}(a_0)$	$\text{Im}(a_1)$	$\text{Im}(a_2)$
$\pi \bar{p}$	S_{11}	1,0+	0.2789	0.1092	0.0148
$\pi \bar{p}$	S_{31}	3,0+	0.0991	-0.0523	0.0136

^aUnits of a_i are fm to the appropriate power. The parameters not listed are zero.

TABLE III

RESONANCE PARAMETERS FOR P_{11} and P_{33} PHASE SHIFTS

Initial State	Spectroscopic Notation	$2I, l\pm$	E_r (fm ⁻¹)	Γ_r (fm ⁻¹)	R (fm)	Γ_{in} (fm ⁻¹)	E_t (fm ⁻¹)	b (fm)
$\pi \bar{p}$	P_{11}	1,1-	7.4487 ^a	1.2669 ^a	0.0 ^a	-	6.1565 ^a	.4176
$\pi \bar{p}$	P_{33}	3,1+	6.2467	0.6109	0.9201	0.0	-	-
$\pi \bar{p}$	P_{33}	3,1+	6.2442	0.5789	1.2290	5.69x 10 ⁻³	-	-

^aThese parameters were not varied in minimizing χ^2 . E_r and Γ_r were taken from "Review of Particle Properties."¹¹

the Coulomb interaction, and are important only in the first few partial waves. The forms used for their interpolation are

$$C_{3,1+} = C_{r3} \arctan\left(\frac{E-E_2}{\Gamma_1/2}\right) / \left[\left(\frac{E-E_1}{\Gamma_1/2}\right)^2 + \frac{E_1-M-m}{E-M-m} \right], \quad (18)$$

$$C_{13,1+} = C_0 + \frac{C_{r13}(\Gamma/2)}{(E-E_1)^2 + (\Gamma/2)^2}, \quad (19)$$

and for the s-wave and remaining p-wave corrections

$$C = C_0 + C_1 k, \quad (20)$$

while the corrections for higher partial waves were ignored. Here m is the rest energy of the pion, E_1 , E_2 , Γ_1 , C_r , C_0 and C_1 are constants. The form given in Eq. (15) is used for Γ simply for convenience. The parameter values for each correction were determined by fitting Eq. (18), Eq. (19), or Eq. (20), as appropriate, to the values used for that correction by Carter, Bugg, and Carter, and are listed in Table IV.

TABLE IV
PARAMETER VALUES FOR $C_{1,\ell\pm}$, $C_{13,\ell\pm}$, and $C_{3,\ell\pm}$

(a) Correction interpolated with Eq. (18)

Partial Wave	$\ell\pm$	Quantity	$C_1(^{\circ})$	$\Gamma_1(\text{fm}^{-1})$	$E_1(\text{fm}^{-1})$	$E_2(\text{fm}^{-1})$
P $3/2$	$1+$	$C_{3,1+}$	1.0779	.4970	.6238	1.0547

(b) Correction interpolated with Eq. (19)

Partial Wave	$\ell\pm$	Quantity	$C_0(^{\circ})$	$C_r(^{\circ})$	$\Gamma_r(\text{fm}^{-1})$	$E_r(\text{fm}^{-1})$
P $3/2$	$1+$	$C_{13,1+}$	-.0607	-.3401	.6848	.7315

(c) Corrections interpolated with Eq. (20)

Partial Wave	$\ell\pm$	Quantity	$C_0(^{\circ})$	$C_1(^{\circ}\text{fm})$
S $1/2$	$0+$	$C_{1,0+}$	-.1284	.0865
		$C_{13,0+}$.0185	.0318
		$C_{3,0+}$.0887	.0569
P $1/2$	$1-$	$C_{1,1-}$.1316	-.1091
		$C_{13,1-}$	-.0393	
		$C_{3,1-}$	-.0282	.0791
P $3/2$	$1+$	$C_{1,1+}$	-.0168	.0434

III. EVALUATION

This section is presented as a guide to the uncertainty one might expect in the predictions of SCATPI. Its predictions are compared with the cross sections calculated from the phase shifts of Carter, Bugg, and Carter, with the measurements included in the analysis of Carter, Bugg, and Carter, and finally with some measurements which have become available since that analysis was completed. For particular applications, one should compare the predictions of SCATPI with the most reliable measurements in the region of interest. The program CROSSEX is also available for this purpose.

A comparison of the predictions of SCATPI with the predictions of Carter, Bugg and Carter is a minimal test of the success of the phase shift interpolation, as well as an indication of the uncertainty of the predictions. For the elastic differential cross section, the two predictions typically differ by 1% for π^+p and 2% for π^-p . The total cross section predictions typically differ by 1/2% for π^+p and 1% for π^-p . The integrated cross section predictions typically differ by 1 3/4% for both π^-p elastic and charge exchange.

A comparison of the predictions of SCATPI with the measurements included in the analysis of Carter, Bugg and Carter is a further test of the interpolation and a more convincing test of the accuracy. In Fig. 1,2 the predictions of SCATPI agree with the measurements of Bussey et al.² for the π^+p differential cross section between 94 and 292 MeV to within the accuracy of the measurements. In Fig. 3, the predictions of SCATPI agree as well as expected with the 310 MeV π^+p angular distribution of Rogers et al.⁵ as renormalized by Carter, Bugg, and Carter; the predictions fall about 3% low at forward angles and 3% high at backward angles, which is substantially the same performance as the predictions from the phase shifts of Carter, Bugg and Carter. In Fig. 4, the predictions of SCATPI for the π^+p polarization at 310 MeV differ systematically by 0.07 from the measurements of Foote et al.⁶ with 0.05 accuracy. In Fig. 5 the predictions of SCATPI also agree with the measurements of Carter et al.,³ for the π^+p total cross section between 90 and 290 MeV, to within the accuracy of the measurements.

For the π^-p differential cross section, the predictions of SCATPI agree with the measurements of Bussey et al.⁴ in Fig. 6-7 between 88 and 260 MeV to within the accuracy of the measurements, and differ with the measurements between 260 and 292 MeV in Fig. 7 by about 3-4%. This lesser agreement between 260 and 292 MeV stems from the difficulty Carter, Bugg, and Carter encountered in the π^-p phase shift analysis above resonance. Between 90 and 290 MeV, the predictions of

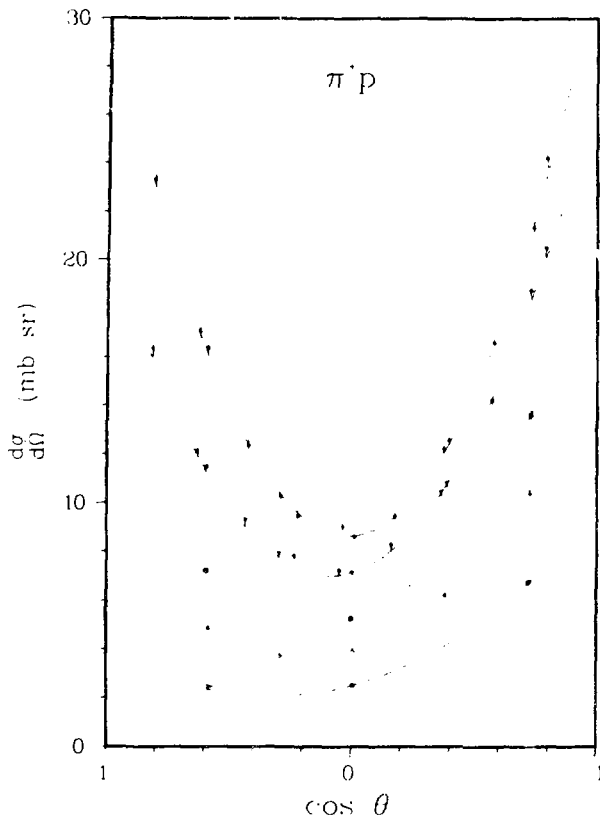


Fig. 1.

Angular distributions of Bussey et al.² for π^+p elastic scattering at lab. energies (0)94.5, (Δ)114.1, (\square)124.8, (∇)142.9, and (\diamond)166.0 MeV. The curves show the predictions of SCATPI excluding Coulomb scattering.

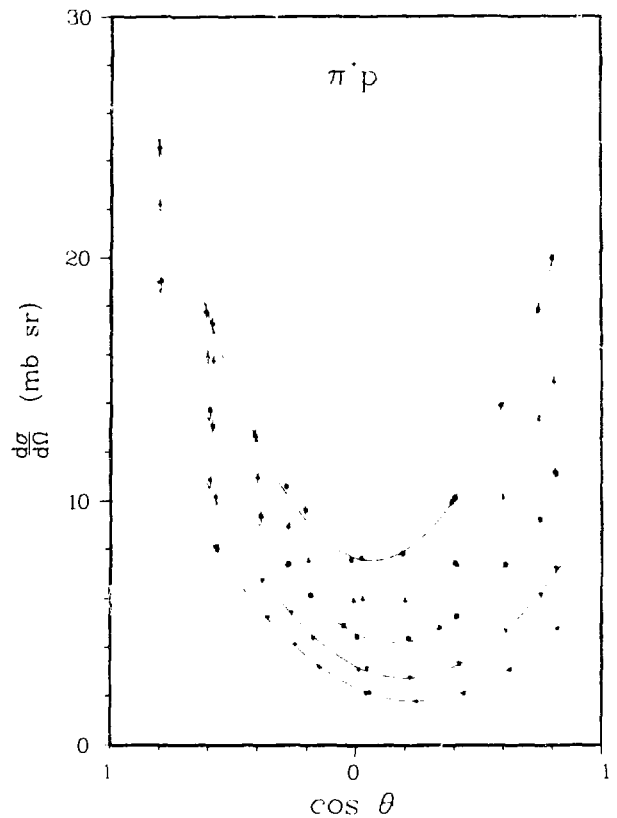


Fig. 2.

Angular distributions of Bussey et al.² for π^+p elastic scattering at lab. energies (0)194.3, (Δ)214.6, (\square)236.3, (∇)263.7, and (\diamond)291.4 MeV. The curves show the predictions of SCATPI excluding Coulomb scattering.

SCATPI in Fig. 8 agree to within 1% with the 1/2% measurement of Carter et al. for the π^-p total cross section, and to within 1 1/2% with the 3/4% measurements of Bugg et al.⁴ for the integrated π^-p charge exchange cross section.

A comparison of the predictions of SCATPI with measurements which have become available since the analysis of Carter, Bugg and Carter is also important in gauging the accuracy of its predictions, but may not test the interpolation of the phase shifts. When discrepancies exist between such measurements and those included in the phase shift analysis, SCATPI will disagree accordingly with measurements not included in the analysis. However, when predictions of SCATPI are supported by subsequent measurements in regions where few measurements were included in the analysis of Carter, Bugg, and Carter, confidence is built in its predictions in these regions. The phase shift analysis at 94.5 MeV included

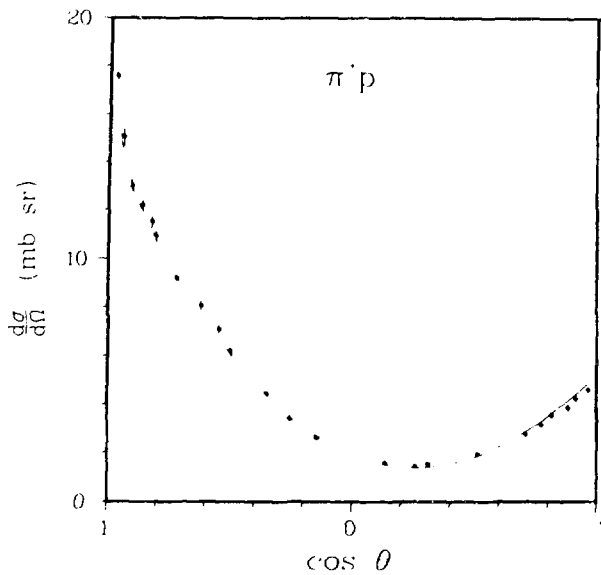


Fig. 3.

Angular distribution of Rogers et al.⁵ for π^+p elastic scattering at lab. energy 310 MeV. The curve shows the predictions of SCATPI including Coulomb scattering.

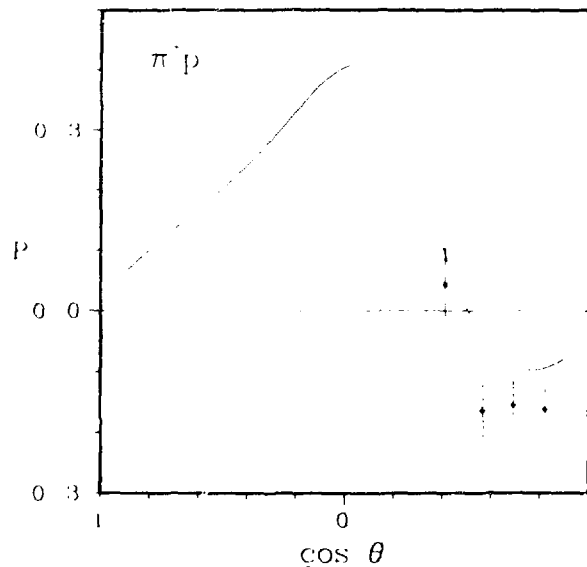


Fig. 4.

Polarization measurements of Forre et al.⁶ for π^+p elastic scattering at lab. energy 310 MeV. The curve shows the predictions of SCATPI including Coulomb scattering.

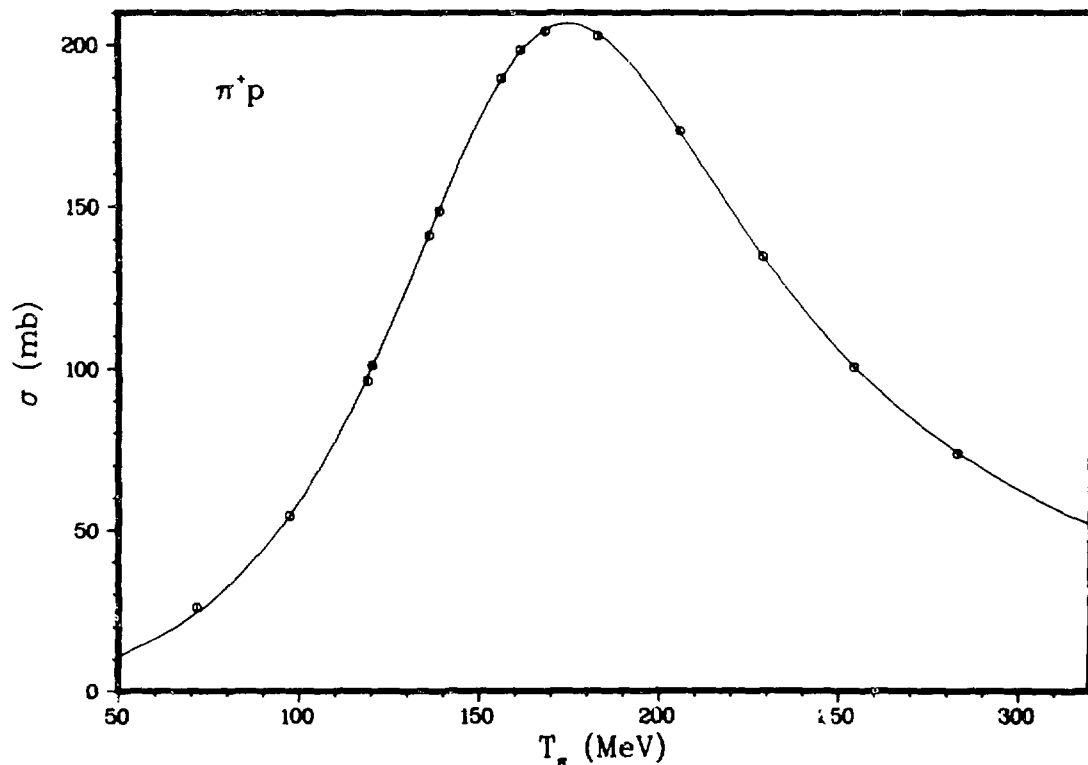


Fig. 5.

Total cross sections of Carter et al.³ for π^+p . The curve shows the predictions of SCATPI.

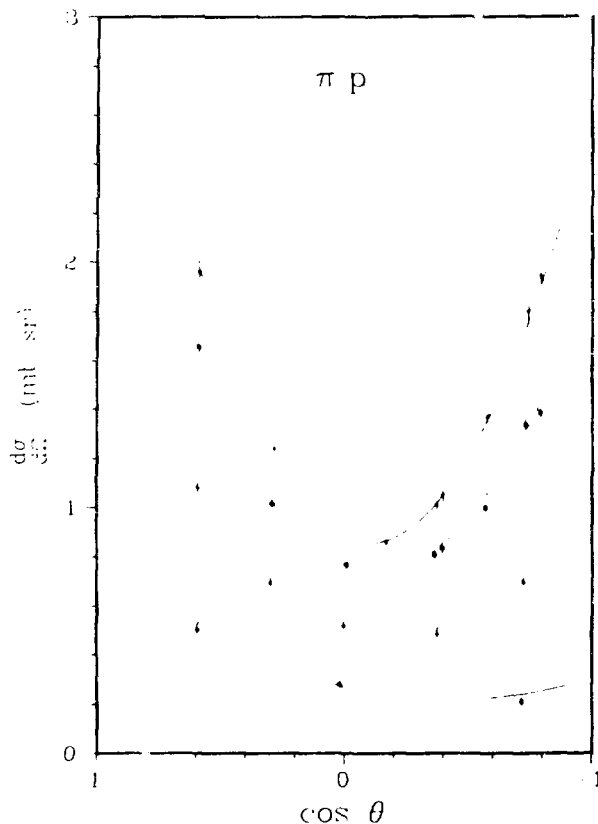


Fig. 6.

Angular distributions of Bussey et al.² for π^+p elastic scattering at lab. energies (○)88.5, (△)119.3, (□)144.2, and (▽)161.9 MeV. The curves show the predictions of SCATPI excluding Coulomb scattering.

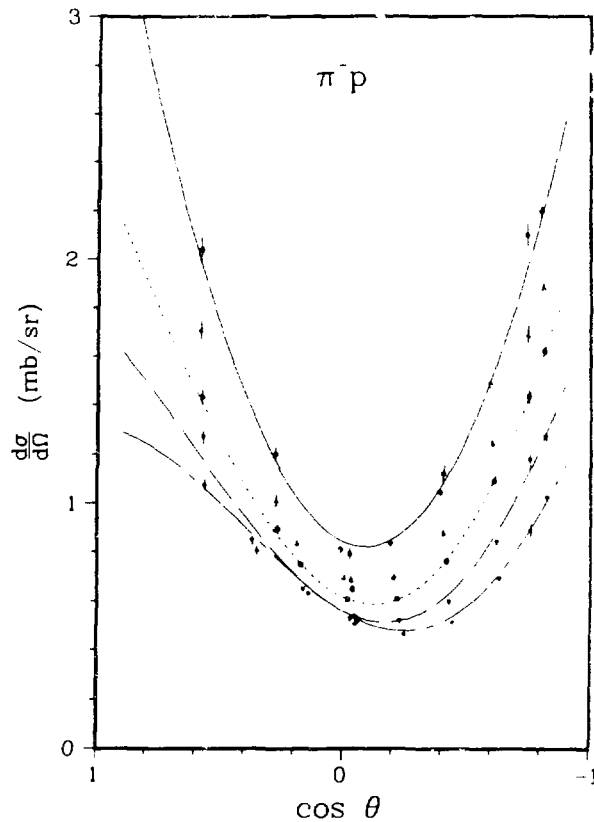


Fig. 7.

Angular distributions of Bussey et al.² for π^-p elastic scattering at lab. energies (○)191.9, (△)219.6, (□)237.9, (▽)253.7, and (◇)291.5 MeV. The curves show the predictions of SCATPI excluding Coulomb scattering.

three values of the π^+p differential cross section and a value for the π^+p total cross section to determine three real phase shifts, and so had only one degree of freedom. In Fig. 9, the predictions of SCATPI for the π^+p differential cross section at 95.9 MeV agree to within 4% with the recent 2% measurements of Bertin et al.¹² Two recent π^+p measurements at 310 MeV are also reassuring. In Fig. 10, the predictions of SCATPI for the polarization agree with the measurements of Dubal et al.¹³ to within the 0.04 measurement uncertainty. In Fig. 11 the predictions of SCATPI for the differential cross section agree with the measurements of Gordeev et al.¹⁴ to within the 3% measurement uncertainty. Although no π^+p polarization measurements below 300 MeV were included in the phase shift analysis, recent measurements give some indication of the reliability here. In Fig. 12, the predictions of SCATPI agree with the polarization measurements of

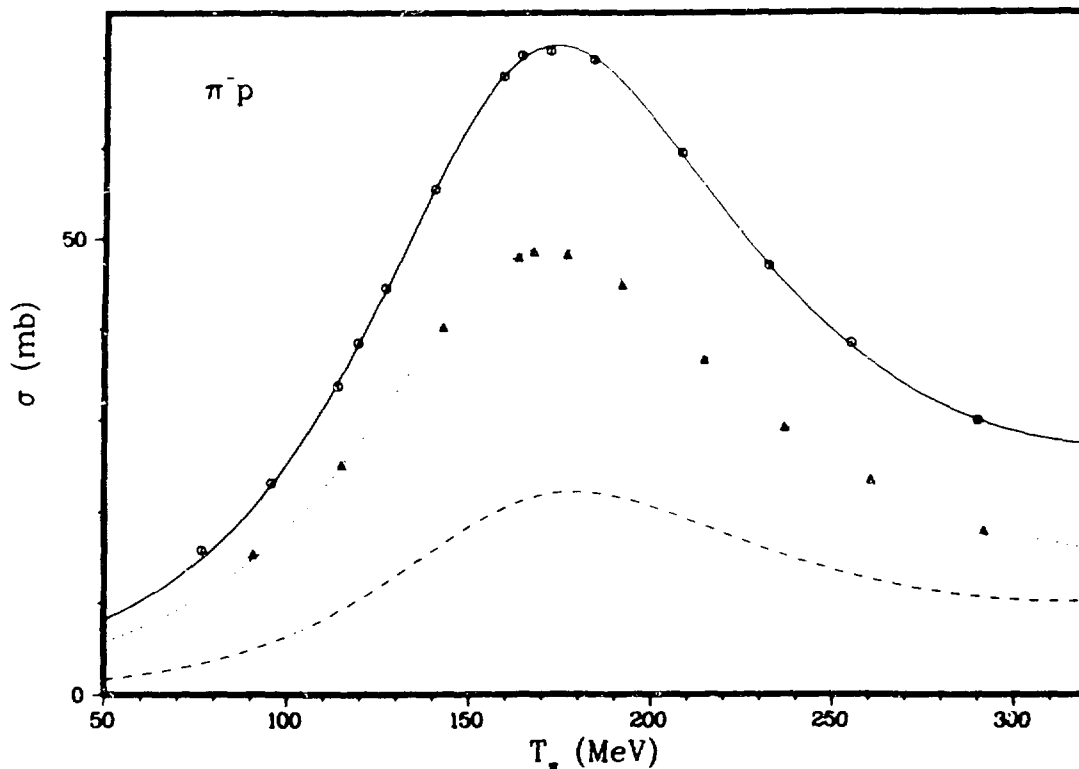


Fig. 8. (O) Total cross sections of Carter et al.³ and (Δ) integrated charge exchange cross sections of Bugg et al.⁴ for π^-p scattering. The curves show the predictions of SCATPI; solid for total cross section, dotted for integrated charge exchange, and dashed for integrated cross section.

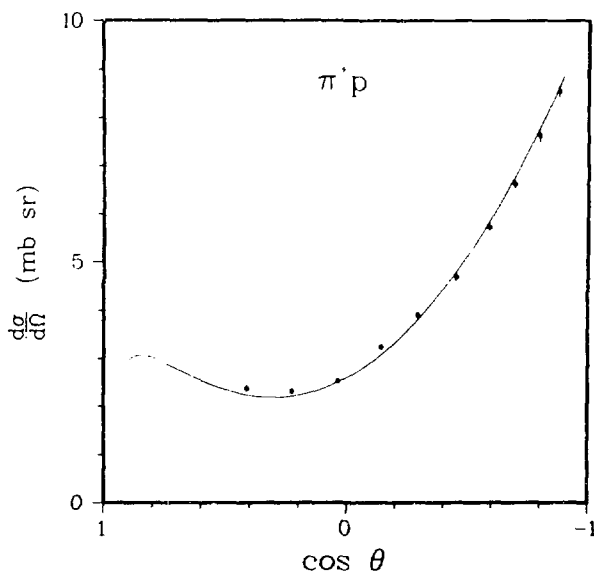


Fig. 9. Angular distribution of Bertin et al.¹² for π^+p elastic scattering at lab. energy 95.9 MeV. The curve shows the predictions of SCATPI including Coulomb scattering.

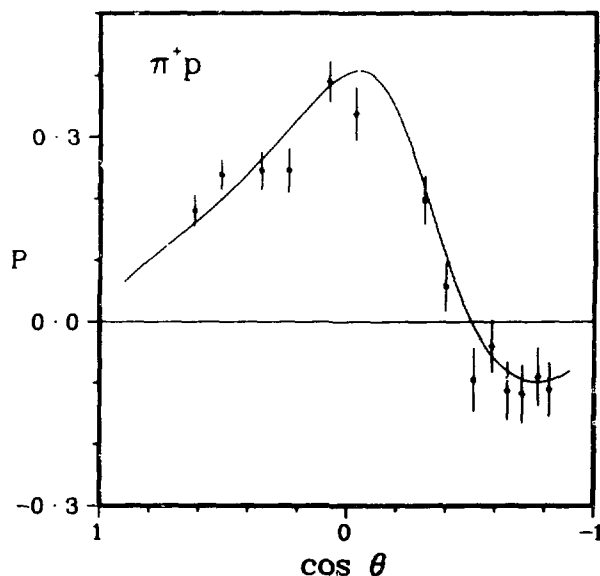


Fig. 10. Polarization measurements of Dubal et al.¹³ for π^+p elastic scattering at lab. energy 308 MeV. The curve shows the predictions of SCATPI including Coulomb scattering.

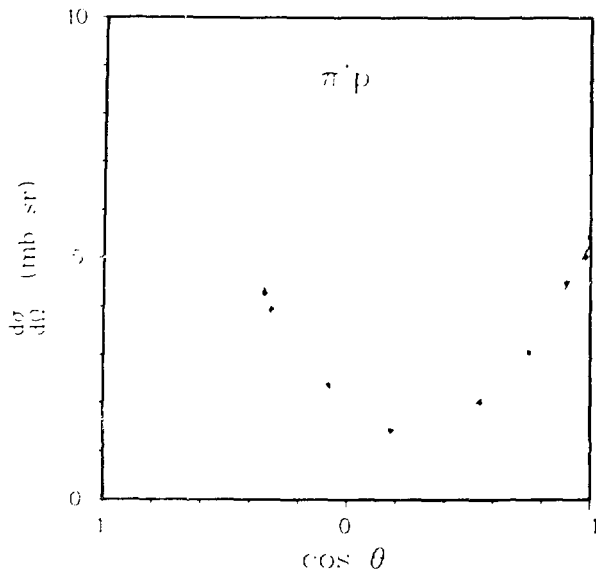


Fig. 11.

Angular distribution of Gordeev et al.¹⁴ for π^+p elastic scattering at lab. energy 308 MeV. The curve shows the predictions of SCATPI including Coulomb scattering.

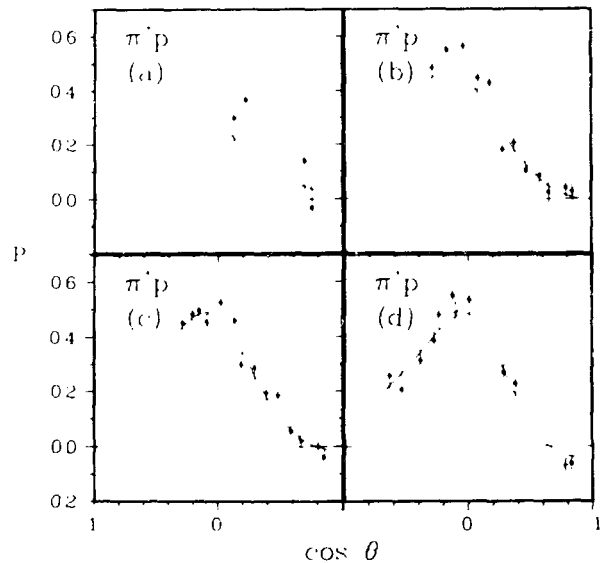


Fig. 12.

Polarization measurements of Amsler et al.¹⁵ for π^+p elastic scattering at lab. energies (a) 94.5 MeV, (b) 166.0 MeV, (c) 194.3 MeV, and (d) 236.3 MeV. The curves show the predictions of SCATPI including Coulomb scattering.

Amsler et al.¹⁵ to within the accuracy of the measurements except possibly at 160 MeV near 90° , where the prediction may be low by about 0.05 to 0.10. The χ^2 for the predictions and these 42 measurements is 44. Finally, recent measurements of the π^+ total cross sections by Pedroni et al.¹⁶ are compared with the predictions of SCATPI. The π^+p total cross sections in Fig. 13 and the π^-p in Fig. 14 agree with the measurements between 165 and 300 MeV, but systematically differ below 165 MeV. The π^+p predictions are 2-3% high, while the π^-p predictions are 2-5% high. These discrepancies are a direct result of the disagreement between the old and new measurements and must be resolved by experiment.

While the performance of the subroutine is generally satisfactory in view of the status of the data and analysis which were input, its precise reliability does depend on the quantity calculated and the energy of the calculation. The importance of checking the predictions of SCATPI with the most reliable measurements in the neighborhood of interest, must, therefore, again be emphasized.

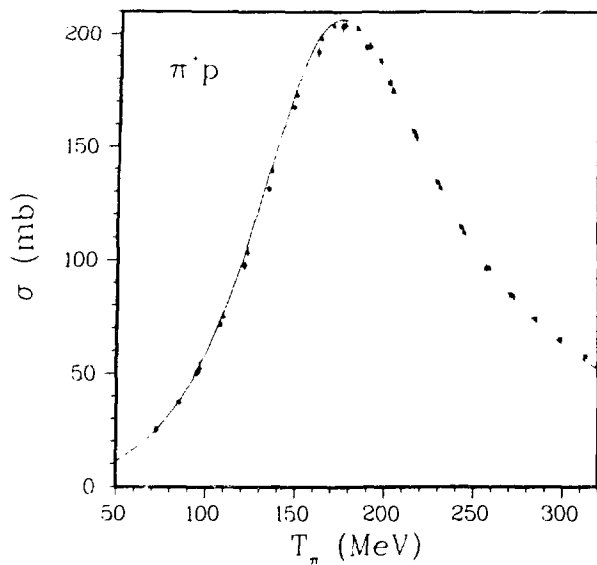


Fig. 13.

Total cross sections of Pedroni et al.¹⁶ for π^+p scattering. The curve shows the predictions of SCATPI.

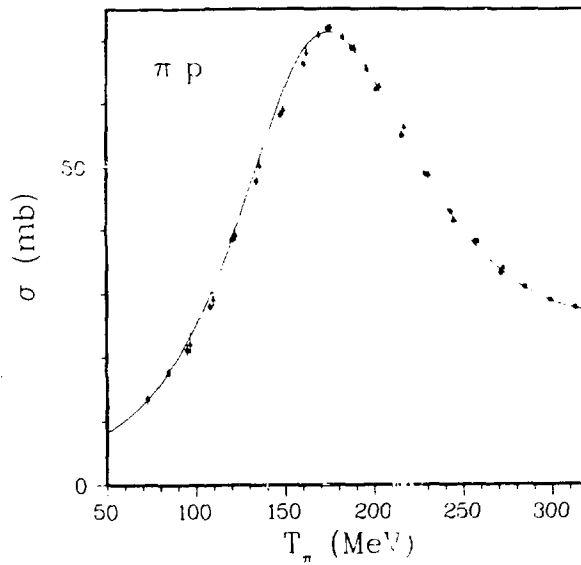


Fig. 14.

Total cross sections of Pedroni et al.¹⁶ for π^-p scattering. The curve shows the predictions of SCATPI.

IV. INSTRUCTIONS FOR USE OF SCATPI

The subroutine SCATPI will compute the scattering amplitudes, differential cross section, and recoil nucleon polarization for charge exchange or elastic scattering from an unpolarized π^+p or π^-p initial state. The differential cross section for a polarized initial state can be constructed from the later two or the former two quantities according to Eq. (2). These calculations can include or exclude Coulomb scattering. SCATPI will also calculate the integrated cross sections and the total cross section excluding Coulomb scattering which is divergent. The calculations are reliable for incident pion energies between 95 and 310 MeV for π^+p , and between 90 and 290 MeV for π^-p elastic scattering, while the reliability for π^-p charge exchange scattering is uncertain.

The general call to SCATPI is

$$\text{CALL SCATPI}(\text{COSCM}, \text{TLAB}, \text{IPI}, \text{ICALC}, \text{IREP}, \text{CALC}, \text{DCALC}) \quad (21)$$

Here COSCM is the cosine of the scattering angle in the center of momentum system, and TLAB is the incident pion kinetic energy in the laboratory system in units of MeV. The initial state and final state are determined by IPI

$$\begin{aligned}
\text{IPI} &= 0 && \text{for } \pi^+p \rightarrow \pi^+p, \\
&= 1 && \text{for } \pi^-p \rightarrow \pi^-p, \\
&= -1 && \text{for } \pi^-p \rightarrow \pi^0n.
\end{aligned}$$

The calculation to be made is determined by the magnitude of ICALC

$$\begin{aligned}
|\text{ICALC}| &= 1 && \text{for the differential cross section,} \\
&= 2 && \text{for the recoil nucleon polarization,} \\
&= 3 && \text{for the integrated cross section,} \\
&= 4 && \text{for the total cross section for the} \\
&&& \text{indicated initial state.}
\end{aligned}$$

For $|\text{ICALC}| = 1$ or 2 , the scattering amplitudes are calculated and are available in the named common block /AMPLTD/ described below. Coulomb scattering is included if $\text{ICALC} < 0$, while it is excluded if $\text{ICALC} > 0$. IREP is an option argument used to save computation time in repeated calculation of the differential cross section and the polarization with the same reaction and incident energy. For

$$\begin{aligned}
\text{IREP} &= 1, && \text{the calculation begins with the} \\
&&& \text{interpolation of the phase shifts,} \\
\text{IREP} &= -1, && \text{the calculation of the phase shifts} \\
&&& \text{is omitted and SCATPI uses the cur-} \\
&&& \text{rent values of the phase shifts,} \\
|\text{IREP}| &> 1, && \text{the calculation of the partial wave} \\
&&& \text{amplitudes is omitted and SCATPI} \\
&&& \text{uses the current values of the partial} \\
&&& \text{wave amplitudes.}
\end{aligned}$$

The second option, $\text{IREP} = -1$, is used to make the calculation with externally supplied phase shifts which are passed through the named common block /PHASE/ described below. Since the $\Delta(1232)$ resonance is treated as charge dependent, it is inadvisable to use $\text{IREP} = -1$ to intersperse π^+p with π^-p calculations. The last option, $|\text{IREP}| > 1$, is used for the second and successive calculations of the scattering amplitudes, differential cross section, or polarization for the same reaction and incident energy. The returned quantities are CALC and DCALC, the calculation and the estimated uncertainty of the calculation, respectively. These

are in mb/sr for the differential cross section, mb for the total and integrated cross sections, and dimensionless for the polarization.

The scattering amplitudes are available, when calculated, through the common block

```
COMMON/AMPLTD/FSTRNG,GSTRNG,FCOUL,GCOUL
```

with FSTRNG and GSTRNG the spin-nonflip and spin-flip amplitudes, respectively, for the strong interaction, given by Eq. (8a) and (8b), and with FCOUL and GCOUL the amplitudes for the Coulomb interaction, given by Eq. (6a) and (6b). These are of course complex. The amplitudes are in $(\text{mb/sr})^{1/2}$.

The phase shifts can be supplied to SCATPI, with IREP = -1, through the common block

```
COMMON/PHASE/PS(6,2,2), PSE(6,2,2),ETA(6,2,2),ETAE(6,2,2),
2 CBC(6,2,2),CBC13(6,2)
```

Here PS and PSE are the real part of the phase shift and its uncertainty, ETA and ETAE are the elasticity and its fractional error, while CBC and CBC13 are the charge dependent phase shifts which are due to the joint action of the Coulomb and strong interactions. In particular,

$$\begin{aligned} \text{PS}(L,M,J) &= \text{Re}(\delta_{2I,\ell\pm}), \\ \text{ETA}(L,M,J) &= \exp(-2 \text{Im}(\delta_{2I,\ell\pm})), \\ \text{CBC}(L,M,J) &= C_{2I,\ell\pm}, \\ \text{CBC13}(L,J) &= C_{13,\ell\pm}, \end{aligned}$$

where $L=\ell+1$, $M=1$ for $I=3/2$ and $M=2$ for $I=1/2$, and $J=1$ for $\ell-$ and $J=2$ for $\ell+$. SCATPI expects PS, PSE, CBC AND CBC13 to be in degrees.

Some examples follow

Example 1

```
CALL SCATPI (DUM,TLAB,1,4,1,SIG,SIGER)
```

SCATPI returns the total cross section SIG in mb for π^-p with an incident kinetic energy TLAB in MeV. SIGER is the calculated uncertainty in SIG and is also in mb. DUM is a dummy argument as the cosine of the scattering angle is not a parameter of the total cross section. The same calculations would be made if IPI, the third argument, were changed to -1 since only the initial state is examined.

Example 2

```
CALL SCATPI(0.5,100.0,0,-2,1,P,PER)
CALL SCATPI(0.5,100.0,0,-1,2,DSIG,DSIGER)
DSIGMA = DSIG*(1.0 + PIN*P*COS(PHI))
```

DSIGMA is the π^+p differential cross section at 100 MeV for a center of momentum scattering angle of 60° , and the angle between the initial state polarization PIN and the normal to the scattering plane $\vec{k}_f \times \vec{k}_i$ being PHI. Note that IREP=2 for the second call to SCATPI since the partial wave amplitudes are the same for both calls and need to be calculated only on the first call. DSIG and hence DSIGMA will be in mb/sr. These quantities and P will include Coulomb scattering since ICALL = -2, -1 is negative for both calls.

Example 3

```
CALL SCATPI (DUM,250.0,-1,3,1,SIG,SIGER)
```

SCATPI returns the integrated charge exchange cross section in SIG in mb for an incident kinetic energy of 250 MeV in the laboratory. SIGER is the calculated uncertainty in SIG and is also in mb. DUM is ignored for the integrated cross section. For

```
CALL SCATPI (DUM,250.0,1,3,1,SIG,SIGER),
```

SIG is the integrated π^-p elastic cross section at 250 MeV.

REFERENCES

1. J. R. Carter, D. V. Bugg, and A. A. Carter, Nucl. Phys. B58, 378 (1973).
2. P. J. Bussey, J. R. Carter, D. R. Dance, D. V. Bugg, A. A. Carter, and A. M. Smith, Nucl. Phys. B58, 363 (1973).
3. A. A. Carter, J. R. Williams, D. V. Bugg, P. J. Bussey, and D. R. Dance, Nucl. Phys. B26, 445 (1971).
4. D. V. Bugg, P. J. Bussey, D. R. Dance, A. R. Smith, A. A. Carter, and J. R. Williams, Nucl. Phys. B26, 588 (1971).
5. E. H. Rogers, O. Chamberlain, J. H. Foote, H. M. Steiner, C. Wiegand, and T. Ypsilantis, Rev. Mod. Phys. 33, 356 (1961).
6. J. H. Foote, O. Chamberlain, E. H. Rogers, H. M. Steiner, C. Wiegand and T. Ypsilantis, Phys. Rev. 122, 948 (1961).
7. L. D. Roper, R. M. Wright and B. T. Feld, Phys. Rev. 138, B190 (1964).
8. P. R. Auvil, Phys. Rev. 168, 1568 (1968); D4, 240 (1971).
9. J. R. Taylor, Scattering Theory (Wiley & Sons, New York, 1972), p. 213-231.
10. J. D. Jackson, Nuovo Cimento 34, 1644 (1964).
11. V. Chaloupka et al., Phys. Lett. 50B, 10 (1974).
12. P. Y. Bertin, B. Coupat, A. Hivernat, D. B. Isabelle, J. Duclos, A. Gerard, J. Miller, J. Morgenstern, J. Picard, P. Vernin, and R. Powers, Nucl. Phys. B106, 341 (1976).
13. L. Dubal, G. H. Eaton, R. Frosch, H. Hirschmann, S. Mango, J. McCulloch, R. Minehart, F. Pozar, U. Rohrer, and P. Wiederkehr, Helv. Phys. Acta 50, 815 (1977).
14. V. A. Gordeev, V. P. Koptev, S. P. Kruglov, L. A. Kuz'min, A. A. Kulbardin, Yu. A. Malov, I. I. Strakovskii, and G. V. Shcherbakov, Yad. Fiz. 24, 1144 (1976) [English transl.: Sov. J. Nucl. Phys. 24, 599 (1977)].
15. C. Amsler, L. Dubal, G. H. Eaton, R. Frosch, S. Mango, F. Pozar and U. Rohrer, Lett. Nuovo Cimento 15, 209 (1976); C. Amsler, F. Rudolf, P. Weymuth, L. Dubal, G. H. Eaton, R. Frosch, S. Mango, and F. Pozar, Phys. Lett. 57B, 289 (1975).
16. E. Pedroni, K. Gabathuler, J. J. Domingo, W. Hirt, P. Schwaller, J. Arvieux, P. Gretillat, J. Piffaretti, N. W. Tanner, and C. Wilkin (to be published).